Acoustic Emission and Acousto-Ultrasonic Monitoring in High Temperature Environments

Luke Pollock and Graham Wild

Abstract: This paper presents a summary of works completed towards the understanding of Acoustic Emission (AE) and Acousto-Ultrasonic (AU) monitoring in high temperature environments. An expanding interest into the development of hypersonic vehicles, operating at Mach numbers greater than five, present challenges with aerodynamic heating at temperatures exceeding 1000 °C. Monitoring of high-risk systems such as turbojet engines operating at high temperatures present similar challenges for vehicles currently in operation. This work comprises a short review of research into the effects of temperature for AE/AU monitoring as well as the Sensors and Actuators (S&As) that may be employed in these environments. A discussion is provided regarding considerations and techniques for the future of in-situ Integrated Vehicular Health Monitoring (IVHM) for AE/AU at high temperatures.

Keywords: SHM, IVHM, AE, AU, Lamb wave, high temperature

Nomenclature

AEs	: Acoustic Emissions
AUs	: Acousto-Ultrasonics
GWs	: Guided Waves
TRL	: Technology Readiness Level
SHM	: Structural Health Monitoring
IVHM	: Integrated Vehicular Health Monitoring
RUL	: Remaining Useful Life
ML	: Machine Learning
OBS	: Optimal Baseline Selection
BSS	: Baseline Signal Stretch
S&As	: Sensors and Acuators
PZT	: Lead Zirconate Titanate
FBG	: Fibre Bragg Grating
LDVR	: Laser Doppler Vibrometer
DT	: Digital Twin
DF	: Data Fusion

1. Introduction

Acoustic Emission (AE) and Acousto-Ultrasonic (AU) Guided Wave (GW) technologies have presented as very realizable methods for the in-situ monitoring of aerospace materials, structures, and systems (Pollock and Wild, 2021, Rose, 2014, Giurgiutiu, 2007). AEs being defined as emissions released natively, typically from a transient event such as crack growth, impact, or from an environmental load. In contrast, AU emissions are characterized as being induced in the material, structure, or system via an actuator, typically an ultrasonic transducer. Whilst the governing behaviour of AE/AU is virtually identical, a distinction is made in this paper to allow for discussion pertaining to the various methods in which such emission can be excited in high temperature environments (Rose, 2014). Of the various GW emissions that may exist, Lamb waves are of particular interest due to their ability to traverse large distances and strong tendencies to interact with damage (Rauter and Lammering, 2015). Due to their extensive application, Lamb waves are the primary focus of this work.

The interrogation of AE/AU in-situ aids towards fulfilling the four main levels of a comprehensive Structural Health Monitoring (SHM) system:

- Level I: The ability to detect damage.
- Level II: The ability to determine the location of damage.
- Level III: The ability to characterize the extent of damage.
- Level IV: The ability to quantify the damage and provide Remaining Useful Life (RUL) assessments.

Unlike alternative methods, AE/AU can fulfil all four levels and are hence, a viable tool towards the creation of SHM. Beyond the interrogation of materials and structures alone and towards the monitoring of systems enables the creation of Integrated Vehicular Health Monitoring (IVHM). IVHM provides an encompassing view of the overall health of the vehicle of which SHM can be considered a part. Individual systems can be effectively monitored, particularly with the use of AEs by examining modal characteristics. The application of Machine Learning (ML) algorithms to large datasets for healthy, baseline operation as well as damaged operation provides the ability to formulate system prognostics and RUL assessment.

IVHM is an effective tool for improving the reliability and performance of aerospace vehicles, particularly for high-risk environments. Development of hypersonic vehicle technologies has accelerated greatly over the past several decades, particularly due to security concerns. Whilst the field has seen deployment of experimental vehicles (~TRL 5), mass production has been delayed, partly owing to the low reliability of some systems (Pollock et al., 2021). The extreme environments in which these vehicles operate introduce large uncertainties and sensitivities of which the use of IVHM can aid in overcoming. Prior to implementation, environmental factors must be considered upon IVHM techniques, of which temperature changes are most notably dominant (Andrews et al., 2008). The operation of vehicles at speeds in excess of Mach five introduces extreme aerodynamic heating that requires consideration and modelling to compensate for in IVHM. High temperatures can also be encountered in subsonic environments, most notably in propulsion systems which have recently been shown as the most common cause of fatigue failure (Pollock et al., 2021).

This paper aims to outline the challenges associated with the deployment of AE/AU based IVHM in high temperature environments as well as the potential methods of overcoming them. Consideration is given for how AE/AU can be performed, including for indirect measurement. A short summary of past works into high temperature AE/AU is provided as well as a discussion regarding potential avenues for future work.

2. Thermal Effects

Early works towards the understanding of thermally induced variations to Lamb wave behaviour focused primarily upon experimental observation. Blaise and Chang (2001) observed reductions in wave amplitudes and phase velocities at temperatures of -90°C. Lee et al. (2003) studied thermal effects on piezoelectric transducer acquired Lamb waves, indicating how the effects of temperature showed dominance to the presence of damage. Amplitude was generally demonstrated as decreasing with increasing temperature. Several methods were proposed to overcome the effects with particular emphasis given towards identifying thermally independent features that could be used for analysis. Works conducted by Lu and Michaels (2005), Michaels and Michaels (2005), and Konstantinidis et al. (2006) attributed the variation in the response of the signals to changes in the physical properties of the materials and hence, dispersion characteristics. Stressed plates, that would arise from thermal gradients, have likewise been shown to exhibit changes in dispersion behaviour (Pei and Bond, 2016).

Whilst a suitable body of literature exists that explores the thermal effects on Lamb wave propagation, little work has been completed at temperatures of interest (> 1000°C). Within this higher temperature range, it is expected that additional phenomena may be encountered that have not been considered in previous work. Materials for use in this temperature range including nickel-based superalloys, titanium aluminides, and Ceramic Matrix Composites (CMCs) exhibit phenomena such as viscoelastic behaviour and creep that has not been characterized or modelled (Ashby et al., 2018). Moreover, accumulation of creep damage results in higher void content and cracking that can further influence AE/AU behaviour and further engenders reflection-transmission responses (Ashby et al., 2018).

2.1. Baseline Methods

In overcoming thermal effects, the most commonly adopted approaches have utilised Optimal Baseline Selection (OBS) or Baseline Signal Stretch (BSS) (Fendzi et al., 2016). The use of OBS relies upon sufficient baseline data from which the most alike baseline is determined from any number of suitable criteria such as least squares error. In comparison, BSS creates a model from acquired baseline data to estimate the change in response. Hence, whilst BSS requires less data to apply, the selection of

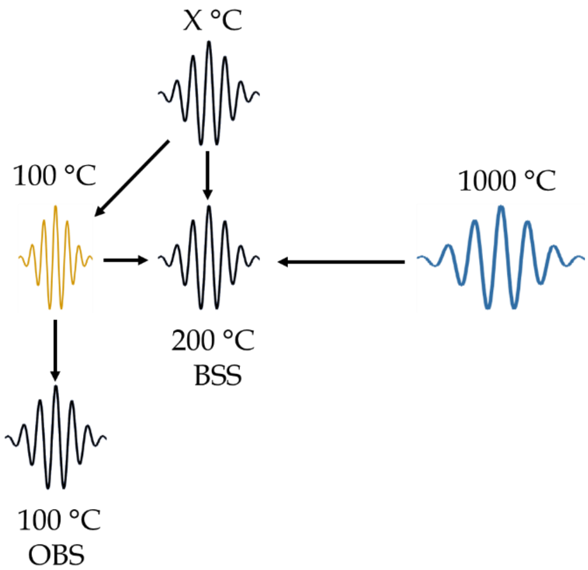

Fig. 1 The difference between the BSS (interpolation) and OBS (nearest neighbour) methods.

suitable modelling methods is of paramount importance. More recently, it has been demonstrated that a combination of OBS and BSS is the most effective method for thermal compensation (Liu et al., 2016). A comparison between OBS and BSS is illustrated in Fig. 1.

A variety of compensation methods have been studied, each with their own merits. Gandhi and Michaels (2010) calculated dispersion curves under the influence of changing physical properties by applying a small linear perturbation to a reference curve. The proposed method was a highly efficient and accurate alternative in comparison to complete recalculation. Clarke et al. (2010) combined OBS and BSS to create a compensation method that required less baseline signals. Fendzi et al. (2016) applied an ordinary least square regression to the thermally induced amplitude factor and phase shift. The two fitted parameters were extracted through application of a Hilbert transform with the model indicating good overall results. Liu et al. (2016) completed similar work by compensating phase shift using a Hilbert transform and amplitude via an orthogonal matching pursuit. The model proved capable up to ±18°C of the baseline signal temperature. Recent work undertaken by Sun et al. (2019) presented an algorithm for Lamb wave compensation across a thermal gradient. Hilbert transform and Levenberg-Marquardt optimization algorithms were used to extract amplitude and phase information from which a model was constructed to estimate compensation parameters.

2.2. Analytical Modelling

Efforts have likewise been made towards analytical modelling to remove the need for the collection of large baseline datasets. One such model developed by Dodson and Inman (2013) is presented below. Similar to the original theory developed by Lamb (1917), the elastic displacement of an infinite, isotropic, and homogenous plate is considered with a traction free boundary condition. However, the physical properties of the plate are given as a function of the temperature change θ and unlike in Lamb's work, are not considered to be constant.

$$(\lambda_T + \mu_T)u_{j,ij} + \mu_T u_{i,jj} + \rho_T f_i = \rho_T \ddot{u}_i \tag{1}$$

Where λ_T and μ_T are the first and second temperature dependent Lamé's constants, respectively. The temperature change θ is taken as the difference between the current temperature T and that of a reference temperature T_0. The half-thickness of the plate h with respect to the thickness at the reference temperature h_0 is then determined by considering the linear coefficient of thermal expansion α.

$$h(\theta) = h_0(1 + \alpha\theta) \tag{2}$$

Likewise, the density of the material with respect to the density at the reference temperature can be determined.

$$\rho(\theta) = \frac{\rho_0}{(1 + \alpha\theta)^3} \tag{3}$$

The variation in Young's modulus and Poisson's ratio were empirically derived by Augereau et al. (2007) for aluminium 6061-T6 over a temperature range of 20°C to 220°C as given below.

$$E = 77.59 - 27.03 \cdot 10^{-3} \cdot T - 13.78 \cdot 10^{-6} \cdot T^2 \tag{4.1}$$

$$\nu = 0.317 + 54.79 \cdot 10^{-3} \cdot T + 6.5 \cdot 10^{-9} \cdot T^2 \tag{4.2}$$

This temperature range, evidently much lower than that being considered as 'high' for the purposes of this work, is a major limitation of the proposed model. Hence, it is noteworthy, that whilst the presented analysis provides a useful analytical framework, empirical models for the temperature-dependent behaviour of materials at higher temperatures are required. Solution of Eq. 1 by application of a Helmholtz decomposition yields the traditional Rayleigh-Lamb equation and indicates that the fundamental behaviour is independent of temperature. Hence, the change in response of the medium to elevated temperatures is solely a product of the change in physical properties. As such, the variation in behaviour may be determined from the p and q constants,

$$p = \sqrt{\frac{\omega^2}{C_L^2(\theta)} - k^2} \tag{5.1}$$

$$q = \sqrt{\frac{\omega^2}{C_T^2(\theta)} - k^2} \tag{5.2}$$

where ω is the angular frequency of the Lamb wave, C_L and C_T are the longitudinal and transverse wave velocities respectively, and k is the Lamb wave number. Taking the derivative of p and q with respect to temperature provides the following relationships.

$$p\frac{\partial p}{\partial T} = k\frac{\partial k}{\partial T} - k_L\frac{\partial k_L}{\partial T} \tag{6.1}$$

$$q\frac{\partial q}{\partial T} = k\frac{\partial k}{\partial T} - k_T\frac{\partial k_T}{\partial T} \tag{6.2}$$

Where k_L and k_T are the longitudinal and transverse wave numbers, respectively. Finally, the group velocity C_G may be calculated as follows from the phase velocity C_P.

$$\frac{\partial C_G}{\partial T} = \frac{\partial C_P}{\partial T}\left(1 - \frac{k}{C_P}\frac{\partial C_P}{\partial k}\right) + k\left(\frac{\partial^2 C_P}{\partial k \partial T}\right) \tag{7}$$

Results of the analytical modelling identified two frequencies of interest for the antisymmetric wave mode that corresponded to no change in the group velocity. These frequencies, identified in Fig. 1, are temperature independent and hence, satisfy Lee et al. (2003) earlier proposed compensation method. Modelling of the

Fig. 1 Group velocity sensitivity reproduced from Dodson and Inman (2013).

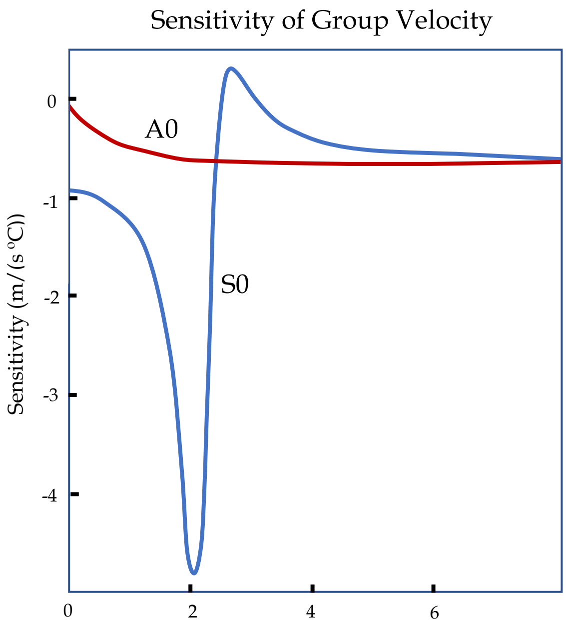

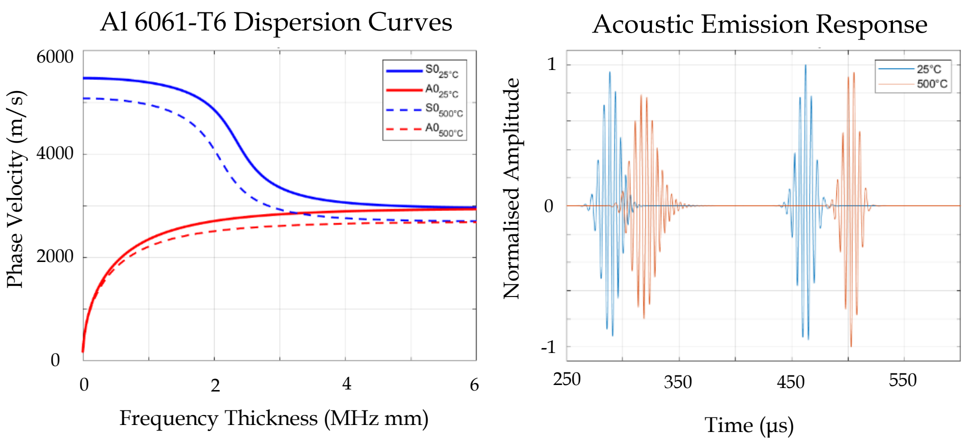

Fig. 22 Thermal effects upon Lamb wave propagation.

thermal variation in phase response of Lamb waves via numerical solutions to the Rayleigh-Lamb equation likewise demonstrate a strong dependence upon temperature. Using the empirical relationships from Augereau et al. (2007), dispersion curves and AEs are computed for aluminium 6061-T6 at 25 ºC and 500 ºC as shown in **Error! Reference source not found.**. As is evident, the change in temperature has a large impact upon the dispersion curves which induce shape and time delay changes to the acquired AEs.

3. Sensors and Actuators (S&As)

Whilst a strong fundamental understanding of AE/AU behaviour is of paramount importance for the interrogation of a structure, there is likewise a requirement for suitable S&As that may be employed at high temperatures. The lack of ability to detect or actuate an emission renders any IVHM system redundant and hence, comparable research is required. Development of suitable S&As may be considered an even more difficult task as the current technology is woefully inadequate for such extreme environments. Piezoelectric lead zirconate titanate (PZT) transducers are the most common due to their ability to function as both sensor and actuator as well as their capability to produce circularly crested waves (Giurgiutiu, 2007). Despite advances towards high temperature PZTs, the current maximum operational limit of such devices remains below 600°C and hence, may only be suitable for the less extreme thermal areas of a structure (Stevenson et al., 2015).

Possibly the only contact sensor technology currently capable of operating in such extreme environments is that of a Fibre Bragg Grating (FBG). FBGs function as a wavelength specific mirror that is etched into an optical fibre cable. Whilst conventional silica fibres have been demonstrated up to 1200°C, single crystalline sapphire in fibre form has been shown capable up to a temperature of 2050°C (Habisreuther et al., 2015). Manufacturing of such fibres is not without challenges however and further work is required to ensure that sensor readings do not drift over time in high temperature environments (Willsch et al., 2009).

Non-contact technologies such as Laser Doppler Vibrometers (LDVRs) (Xiao and Yu, 2019) and high-power laser pulse actuators (Hosoya et al., 2018) show potential promise. However, a direct line of sight to the surface is required. Moreover, sufficient space is required between surface and sensor or actuator to limit thermal radiation. Hence, in the application of AE monitoring, the use of silica or sapphire FBGs may prove sufficient, however, there does not yet exist a suitable method for the ultrasonic transduction required for AU methods.

4. Conclusion

Ultimately, it is evident that further work is required towards both the understanding of AE/AU behaviour at high temperatures as well as for the development of S&As capable of enduring such extreme environments. Alternative methods to overcome physical limitations may see the application of non-contact technologies, however, Digital Twin (DT) techniques may prove equally useful. The development of a suitably accurate DT model renders the ability to gather numerical and simulation data. Environmental inputs to the DT can be sourced from sensor networks and used to predict the system response. Moreover, whilst few S&As exist that are suitable for the extrema conditions, instrumentation may be employed in a reasonable proximity to the region of interest following which an appropriate Data Fusion (DF) algorithm may be applied. A combination of experimental and numerically simulated data from the DT model combined using a DF technique such as a Kalman filter or neural network aims to enhance the reliability of the IVHM system without the need for direct contact monitoring.

Moreover, the use of ML may be used to aid in the selection of suitable baseline for thermal compensation and with adequate data may also aid in overcoming the viscoelastic and creep responses of the material. More work is evidently required to fully realise the potential applications of AE/AU IVHM in which the possibility for complete implementation has the potential to drastically increase the reliability of systems operating in extreme environments.

References

Andrews, J. P., Palazotto, A. N., DeSimio, M. P. & Olson, S. E. 2008. Lamb wave propagation in varying isothermal environments. Structural Health Monitoring, 7, p. 265-270.

Ashby, M. F., Shercliff, H. & Cebon, D. 2018. Materials: engineering, science, processing and design, Butterworth-Heinemann.

Augereau, F., Laux, D., Allais, L., Mottot, M. & Caes, C. 2007. Ultrasonic measurement of anisotropy and temperature dependence of elastic parameters by a dry coupling method applied to a 6061-T6 alloy. Ultrasonics, 46, p. 34-41.

Blaise, E. & Chang, F. Built-in diagnostics for debonding in sandwich structures under extreme temperatures. Proceedings of the 3rd international workshop on structural health monitoring, 2001. Stanford, California, USA, p. 154-163.

Clarke, T., Simonetti, F. & Cawley, P. 2010. Guided wave health monitoring of complex structures by sparse array systems: Influence of temperature changes on performance. Journal of Sound and Vibration, 329, p. 2306-2322.

Dodson, J. & Inman, D. 2013. Thermal sensitivity of Lamb waves for structural health monitoring applications. Ultrasonics, 53, p. 677-685.

Fendzi, C., Rebillat, M., Mechbal, N., Guskov, M. & Coffignal, G. 2016. A data-driven temperature compensation approach for Structural Health Monitoring using Lamb waves. Structural Health Monitoring, 15, p. 525-540.

Gandhi, N. & Michaels, J. E. Efficient perturbation analysis of Lamb wave dispersion curves. AIP Conference Proceedings, 2010. American Institute of Physics, p. 215-222.

Giurgiutiu, V. 2007. Structural health monitoring: with piezoelectric wafer active sensors, Elsevier.

Habisreuther, T., Elsmann, T., Pan, Z., Graf, A., Willsch, R. & Schmidt, M. A. 2015. Sapphire fiber Bragg gratings for high temperature and dynamic temperature diagnostics. Applied Thermal Engineering, 91, p. 860-865.

Hosoya, N., Yoshinaga, A., Kanda, A. & Kajiwara, I. 2018. Non-contact and non-destructive Lamb wave generation using laser-induced plasma shock wave. International journal of mechanical sciences, 140, p. 486-492.

Konstantinidis, G., Drinkwater, B. W. & Wilcox, P. D. 2006. The temperature stability of guided wave structural health monitoring systems. Smart Materials and Structures, 15, p. 967.

Lamb, H. 1917. On waves in an elastic plate. Proceedings of the Royal Society of London. Series A, Containing papers of a mathematical and physical character, 93, p. 114-128.

Lee, B., Manson, G. & Staszewski, W. Environmental effects on Lamb wave responses from piezoceramic sensors. Materials Science Forum, 2003. Trans Tech Publ, p. 195-202.

Liu, G., Xiao, Y., Zhang, H. & Ren, G. 2016. Baseline signal reconstruction for temperature compensation in lamb wave-based damage detection. Sensors, 16, p. 1273.

Lu, Y. & Michaels, J. E. 2005. A methodology for structural health monitoring with diffuse ultrasonic waves in the presence of temperature variations. Ultrasonics, 43, p. 717-731.

Michaels, J. E. & Michaels, T. E. 2005. Detection of structural damage from the local temporal coherence of diffuse ultrasonic signals. IEEE transactions on ultrasonics, ferroelectrics, and frequency control, 52, p. 1769-1782.

Pei, N. & Bond, L. J. 2016. Higher order acoustoelastic Lamb wave propagation in stressed plates. The Journal of the Acoustical Society of America, 140, p. 3834-3843.

Pollock, L. & Wild, G. 2021. Spectral Domain Analysis of Acousto-Ultrasonic Tone Burst Lamb Wave Emissions in Uncured Pre-Preg Carbon Fiber Composites. AIAA ASCEND. Las Vegas, Nevada: AIAA.

Pollock, L., Wild, G., Abdelwahab, A. K. & Murray, J. 2021. The Need for Aerospace Structural Health Monitoring: A review of aircraft fatigue accidents. International Journal of Prognostics and Health Management, 12, p.

Rauter, N. & Lammering, R. 2015. Impact damage detection in composite structures considering nonlinear lamb wave propagation. Mechanics of Advanced Materials and Structures, 22, p. 44-51.

Rose, J. L. 2014. Ultrasonic guided waves in solid media, Cambridge university press.

Stevenson, T., Martin, D., Cowin, P., Blumfield, A., Bell, A., Comyn, T. & Weaver, P. 2015. Piezoelectric materials for high temperature transducers and actuators. Journal of Materials Science: Materials in Electronics, 26, p. 9256-9267.

Sun, H., Yi, J., Xu, Y., Wang, Y. & Qing, X. 2019. Identification and compensation technique of non-uniform temperature field for Lamb wave-and multiple sensors-based damage detection. Sensors, 19, p. 2930.

Willsch, M., Bosselmann, T., Flohr, P., Kull, R., Ecke, W., Latka, I., Fischer, D. & Thiel, T. Design of fiber optical high temperature sensors for gas turbine monitoring. 20th International Conference on Optical Fibre Sensors, 2009. International Society for Optics and Photonics, p. 75037R.

Xiao, W. & Yu, L. Nondestructive evaluation with fully non-contact air-coupled transducer-scanning laser Doppler vibrometer Lamb wave system. Nondestructive Characterization and Monitoring of Advanced Materials, Aerospace, Civil Infrastructure, and Transportation XIII, 2019. International Society for Optics and Photonics, p. 109711G.